



**Measurement of the Decay Amplitudes of
 $B^0 \rightarrow J/\psi K^{*0}$ and $B_s^0 \rightarrow J/\psi \phi$ Decays**

T. Affolder,²¹ H. Akimoto,⁴³ A. Akopian,³⁶ M. G. Albrow,¹⁰ P. Amaral,⁷ S. R. Amendolia,³² D. Amidei,²⁴ K. Anikeev,²² J. Antos,¹ G. Apolinari,¹⁰ T. Arisawa,⁴³ T. Asakawa,⁴¹ W. Ashmanskas,⁷ M. Atac,¹⁰ F. Azfar,²⁹ P. Azzi-Bacchetta,³⁰ N. Bacchetta,³⁰ M. W. Bailey,²⁶ S. Bailey,¹⁴ P. de Barbaro,³⁵ A. Barbaro-Galtieri,²¹ V. E. Barnes,³⁴ B. A. Barnett,¹⁷ M. Barone,¹² G. Bauer,²² F. Bedeschi,³² S. Belforte,⁴⁰ G. Bellettini,³² J. Bellinger,⁴⁴ D. Benjamin,⁹ J. Bensinger,⁴ A. Beretvas,¹⁰ J. P. Berge,¹⁰ J. Berryhill,⁷ B. Bevensee,³¹ A. Bhatti,³⁶ M. Binkley,¹⁰ D. Bisello,³⁰ R. E. Blair,² C. Blocker,⁴ K. Bloom,²⁴ B. Blumenfeld,¹⁷ S. R. Blusk,³⁵ A. Bocci,³² A. Bodek,³⁵ W. Bokhari,³¹ G. Bolla,³⁴ Y. Bonushkin,⁵ D. Bortoletto,³⁴ J. Boudreau,³³ A. Brandl,²⁶ S. van den Brink,¹⁷ C. Bromberg,²⁵ M. Brozovic,⁹ N. Bruner,²⁶ E. Buckley-Geer,¹⁰ J. Budagov,⁸ H. S. Budd,³⁵ K. Burkett,¹⁴ G. Busetto,³⁰ A. Byon-Wagner,¹⁰ K. L. Byrum,² P. Calafiura,²¹ M. Campbell,²⁴ W. Carithers,²¹ J. Carlson,²⁴ D. Carlsmith,⁴⁴ J. Cassada,³⁵ A. Castro,³⁰ D. Cauz,⁴⁰ A. Cerri,³² A. W. Chan,¹ P. S. Chang,¹ P. T. Chang,¹ J. Chapman,²⁴ C. Chen,³¹ Y. C. Chen,¹ M. -T. Cheng,¹ M. Chertok,³⁸ G. Chiarelli,³² I. Chirikov-Zorin,⁸ G. Chlachidze,⁸ F. Chlebana,¹⁰ L. Christofek,¹⁶ M. L. Chu,¹ Y. S. Chung,³⁵ C. I. Ciobanu,²⁷ A. G. Clark,¹³ A. Connolly,²¹ J. Conway,³⁷ J. Cooper,¹⁰ M. Cordelli,¹² J. Cranshaw,³⁹ D. Cronin-Hennessy,⁹ R. Cropp,²³ R. Culbertson,⁷ D. Dagenhart,⁴² F. DeJongh,¹⁰ S. Dell'Agnello,¹² M. Dell'Orso,³² R. Demina,¹⁰ L. Demortier,³⁶ M. Deninno,³ P. F. Derwent,¹⁰ T. Devlin,³⁷ J. R. Dittmann,¹⁰ S. Donati,³² J. Done,³⁸ T. Dorigo,¹⁴ N. Eddy,¹⁶ K. Einsweiler,²¹ J. E. Elias,¹⁰ E. Engels, Jr.,³³ W. Erdmann,¹⁰ D. Errede,¹⁶ S. Errede,¹⁶ Q. Fan,³⁵ R. G. Feild,⁴⁵ C. Ferretti,³² R. D. Field,¹¹ I. Fiori,³ B. Flaugher,¹⁰ G. W. Foster,¹⁰ M. Franklin,¹⁴ J. Freeman,¹⁰ J. Friedman,²² Y. Fukui,²⁰ I. Furic,²² S. Galeotti,³² M. Gallinaro,³⁶ T. Gao,³¹ M. Garcia-Sciveres,²¹ A. F. Garfinkel,³⁴ P. Gatti,³⁰ C. Gay,⁴⁵ S. Geer,¹⁰ D. W. Gerdes,²⁴ P. Giannetti,³² P. Giromini,¹² V. Glagolev,⁸ M. Gold,²⁶ J. Goldstein,¹⁰ A. Gordon,¹⁴ A. T. Goshaw,⁹ Y. Gotra,³³ K. Goulianatos,³⁶ C. Green,³⁴ L. Groer,³⁷ C. Grossos-Pilcher,⁷ M. Guenther,³⁴ G. Guilliam,²⁴ J. Guimaraes da Costa,¹⁴ R. S. Guo,¹ R. M. Haas,¹¹ C. Haber,²¹ E. Hafner,²² S. R. Hahn,¹⁰ C. Hall,¹⁴ T. Handa,¹⁵ R. Handler,⁴⁴ W. Hao,³⁹ F. Happacher,¹² K. Hara,⁴¹ A. D. Hardman,³⁴ R. M. Harris,¹⁰ F. Hartmann,¹⁸ K. Hatakeyama,³⁶ J. Hauser,⁵ J. Heinrich,³¹ A. Heiss,¹⁸ M. Herndon,¹⁷ K. D. Hoffman,³⁴ C. Holck,³¹ R. Hollebeek,³¹ L. Holloway,¹⁶ R. Hughes,²⁷ J. Huston,²⁵ J. Huth,¹⁴ H. Ikeda,⁴¹ J. Incandela,¹⁰ G. Introzzi,³² J. Iwai,⁴³ Y. Iwata,¹⁵ E. James,²⁴ H. Jensen,¹⁰ M. Jones,³¹ U. Joshi,¹⁰ H. Kambara,¹³ T. Kamon,³⁸ T. Kaneko,⁴¹ K. Karr,⁴² H. Kasha,⁴⁵ Y. Kato,²⁸ T. A. Keaffaber,³⁴ K. Kelley,²² M. Kelly,²⁴ R. D. Kennedy,¹⁰ R. Kephart,¹⁰ D. Khazins,⁹ T. Kikuchi,⁴¹ B. Kilminster,³⁵ M. Kirby,⁹ M. Kirk,⁴ B. J. Kim,¹⁹ D. H. Kim,¹⁹ H. S. Kim,¹⁶ M. J. Kim,¹⁹ S. H. Kim,⁴¹ Y. K. Kim,²¹ L. Kirsch,⁴ S. Klimentko,¹¹ P. Koehn,²⁷ A. Kongeter,¹⁸ K. Kondo,⁴³ J. Konigsberg,¹¹ K. Kordas,²³ A. Korn,²² A. Korytov,¹¹ E. Kovacs,² J. Kroll,³¹ M. Kruse,³⁵ S. E. Kuhlmann,² K. Kurino,¹⁵ T. Kuwabara,⁴¹ A. T. Laasanen,³⁴ N. Lai,⁷ S. Lami,³⁶ S. Lammel,¹⁰ J. I. Lamoureux,⁴ M. Lancaster,²¹ G. Latino,³² T. LeCompte,² A. M. Lee IV,⁹ K. Lee,³⁹ S. Leone,³² J. D. Lewis,¹⁰ M. Lindgren,⁵ T. M. Liss,¹⁶ J. B. Liu,³⁵ Y. C. Liu,¹ N. Lockyer,³¹ J. Loken,²⁹ M. Loretto,³⁰ D. Lucchesi,³⁰ P. Lukens,¹⁰ S. Lusin,⁴⁴ L. Lyons,²⁹ J. Lys,²¹ R. Madrak,¹⁴ K. Maeshima,¹⁰ P. Maksimovic,¹⁴ L. Malferrari,³ M. Mangano,³² M. Mariotti,³⁰ G. Martignon,³⁰ A. Martin,⁴⁵ J. A. J. Matthews,²⁶ J. Mayer,²³ P. Mazzanti,³ K. S. McFarland,³⁵ P. McIntyre,³⁸ E. McKigney,³¹ M. Menguzzato,³⁰ A. Menzione,³² C. Mesropian,³⁶ A. Meyer,⁷ T. Miao,¹⁰ R. Miller,²⁵ J. S. Miller,²⁴ H. Minato,⁴¹ S. Miscetti,¹² M. Mishina,²⁰ G. Mitselmakher,¹¹ N. Moggi,³ E. Moore,²⁶ R. Moore,²⁴ Y. Morita,²⁰ M. Mulhearn,²² A. Mukherjee,¹⁰ T. Muller,¹⁸ A. Munar,³² P. Murat,¹⁰ S. Murgia,²⁵ M. Musy,⁴⁰ J. Nachtman,⁵ S. Nahm,⁴⁵ H. Nakada,⁴¹ T. Nakaya,⁷ I. Nakano,¹⁵ C. Nelson,¹⁰ D. Neuberger,¹⁸ C. Newman-Holmes,¹⁰ C.-Y. P. Ngan,²² P. Nicolaidi,⁴⁰ H. Niu,⁴ L. Nodulman,² A. Nomerotski,¹¹ S. H. Oh,⁹ T. Ohmoto,¹⁵ T. Ohsugi,¹⁵ R. Oishi,⁴¹ T. Okusawa,²⁸ J. Olsen,⁴⁴ W. Orejudos,²¹ C. Pagliarone,³² F. Palmonari,³² R. Paoletti,³² V. Papadimitriou,³⁹ S. P. Pappas,⁴⁵ D. Partos,⁴ J. Patrick,¹⁰ G. Paoletta,⁴⁰ M. Paulini,²¹ C. Paus,²² L. Pescara,³⁰ T. J. Phillips,⁹ G. Piacentino,³² K. T. Pitts,¹⁶ R. Plunkett,¹⁰ A. Pompos,³⁴ L. Pondrom,⁴⁴ G. Pope,³³ M. Popovic,²³ F. Prokoshin,⁸ J. Proudfoot,² F. Ptahos,¹² O. Pukhov,⁸ G. Punzi,³² K. Ragan,²³ A. Rakitine,²² D. Reher,²¹ A. Reichold,²⁹ W. Riegler,¹⁴ A. Ribon,³⁰ F. Rimondi,³ L. Ristori,³² M. Riveline,²³ W. J. Robertson,⁹ A. Robinson,²³ T. Rodrigo,⁶ S. Rolli,⁴² L. Rosenson,²² R. Roser,¹⁰ R. Rossin,³⁰ A. Safonov,³⁶ W. K. Sakumoto,³⁵ D. Saltzberg,⁵ A. Sansoni,¹² L. Santi,⁴⁰ H. Sato,⁴¹ P. Savard,²³ P. Schlabach,¹⁰ E. E. Schmidt,¹⁰ M. P. Schmidt,⁴⁵ M. Schmitt,¹⁴ L. Scodellaro,³⁰ A. Scott,⁵ A. Scribano,³² S. Segler,¹⁰ S. Seidel,²⁶ Y. Seiya,⁴¹ A. Semenov,⁸ F. Semeria,³ T. Shah,²² M. D. Shapiro,²¹ P. F. Shepard,³³ T. Shibayama,⁴¹ M. Shimojima,⁴¹ M. Shochet,⁷ J. Siegrist,²¹ G. Signorelli,³² A. Sill,³⁹ P. Sinervo,²³ P. Singh,¹⁶ A. J. Slaughter,⁴⁵ K. Sliwa,⁴² C. Smith,¹⁷ F. D. Snider,¹⁰ A. Solodsky,³⁶ J. Spalding,¹⁰ T. Speer,¹³ P. Sphicas,²² F. Spinella,³² M. Spiropulu,¹⁴ L. Spiegel,¹⁰ J. Steele,⁴⁴ A. Stefanini,³² J. Strologas,¹⁶ F. Strumia,¹³ D. Stuart,¹⁰ K. Sumorok,²²

T. Suzuki,⁴¹ T. Takano,²⁸ R. Takashima,¹⁵ K. Takikawa,⁴¹ P. Tamburello,⁹ M. Tanaka,⁴¹ B. Tannenbaum,⁵
 W. Taylor,²³ M. Tecchio,²⁴ P. K. Teng,¹ K. Terashi,³⁶ S. Tether,²² D. Theriot,¹⁰ R. Thurman-Keup,² P. Tipton,³⁵
 S. Tkaczyk,¹⁰ K. Tollefson,³⁵ A. Tollesstrup,¹⁰ H. Toyoda,²⁸ W. Trischuk,²³ J. F. de Troconiz,¹⁴ J. Tseng,²²
 N. Turini,³² F. Ukegawa,⁴¹ T. Vaiciulis,³⁵ J. Valls,³⁷ S. Vejcik III,¹⁰ G. Velev,¹⁰ R. Vidal,¹⁰ R. Vilar,⁶
 I. Volobouev,²¹ D. Vucinic,²² R. G. Wagner,² R. L. Wagner,¹⁰ J. Wahl,⁷ N. B. Wallace,³⁷ A. M. Walsh,³⁷ C. Wang,⁹
 C. H. Wang,¹ M. J. Wang,¹ T. Watanabe,⁴¹ D. Waters,²⁹ T. Watts,³⁷ R. Webb,³⁸ H. Wenzel,¹⁸ W. C. Wester III,¹⁰
 A. B. Wicklund,² E. Wicklund,¹⁰ H. H. Williams,³¹ P. Wilson,¹⁰ B. L. Winer,²⁷ D. Winn,²⁴ S. Wolbers,¹⁰
 D. Wolinski,²⁴ J. Wolinski,²⁵ S. Wolinski,²⁴ S. Worm,²⁶ X. Wu,¹³ J. Wyss,³² A. Yagil,¹⁰ W. Yao,²¹ G. P. Yeh,¹⁰
 P. Yeh,¹ J. Yoh,¹⁰ C. Yosef,²⁵ T. Yoshida,²⁸ I. Yu,¹⁹ S. Yu,³¹ Z. Yu,⁴⁵ A. Zanetti,⁴⁰ F. Zetti,²¹ and S. Zucchelli³

(CDF Collaboration)

¹ *Institute of Physics, Academia Sinica, Taipei, Taiwan 11529, Republic of China*

² *Argonne National Laboratory, Argonne, Illinois 60439*

³ *Istituto Nazionale di Fisica Nucleare, University of Bologna, I-40127 Bologna, Italy*

⁴ *Brandeis University, Waltham, Massachusetts 02254*

⁵ *University of California at Los Angeles, Los Angeles, California 90024*

⁶ *Instituto de Fisica de Cantabria, CSIC-University of Cantabria, 39005 Santander, Spain*

⁷ *Enrico Fermi Institute, University of Chicago, Chicago, Illinois 60637*

⁸ *Joint Institute for Nuclear Research, RU-141980 Dubna, Russia*

⁹ *Duke University, Durham, North Carolina 27708*

¹⁰ *Fermi National Accelerator Laboratory, Batavia, Illinois 60510*

¹¹ *University of Florida, Gainesville, Florida 32611*

¹² *Laboratori Nazionali di Frascati, Istituto Nazionale di Fisica Nucleare, I-00044 Frascati, Italy*

¹³ *University of Geneva, CH-1211 Geneva 4, Switzerland*

¹⁴ *Harvard University, Cambridge, Massachusetts 02138*

¹⁵ *Hiroshima University, Higashi-Hiroshima 734, Japan*

¹⁶ *University of Illinois, Urbana, Illinois 61801*

¹⁷ *The Johns Hopkins University, Baltimore, Maryland 21218*

¹⁸ *Institut für Experimentelle Kernphysik, Universität Karlsruhe, 76128 Karlsruhe, Germany*

¹⁹ *Korean Hadron Collider Laboratory: Kyungpook National University, Taegu 702-701; Seoul National University, Seoul 151-742; and SungKyunKwan University, Suwon 440-746; Korea*

²⁰ *High Energy Accelerator Research Organization (KEK), Tsukuba, Ibaraki 305, Japan*

²¹ *Ernest Orlando Lawrence Berkeley National Laboratory, Berkeley, California 94720*

²² *Massachusetts Institute of Technology, Cambridge, Massachusetts 02139*

²³ *Institute of Particle Physics: McGill University, Montreal H3A 2T8; and University of Toronto, Toronto M5S 1A7; Canada*

²⁴ *University of Michigan, Ann Arbor, Michigan 48109*

²⁵ *Michigan State University, East Lansing, Michigan 48824*

²⁶ *University of New Mexico, Albuquerque, New Mexico 87131*

²⁷ *The Ohio State University, Columbus, Ohio 43210*

²⁸ *Osaka City University, Osaka 588, Japan*

²⁹ *University of Oxford, Oxford OX1 3RH, United Kingdom*

³⁰ *Università di Padova, Istituto Nazionale di Fisica Nucleare, Sezione di Padova, I-35131 Padova, Italy*

³¹ *University of Pennsylvania, Philadelphia, Pennsylvania 19104*

³² *Istituto Nazionale di Fisica Nucleare, University and Scuola Normale Superiore di Pisa, I-56100 Pisa, Italy*

³³ *University of Pittsburgh, Pittsburgh, Pennsylvania 15260*

³⁴ *Purdue University, West Lafayette, Indiana 47907*

³⁵ *University of Rochester, Rochester, New York 14627*

³⁶ *Rockefeller University, New York, New York 10021*

³⁷ *Rutgers University, Piscataway, New Jersey 08855*

³⁸ *Texas A&M University, College Station, Texas 77843*

³⁹ *Texas Tech University, Lubbock, Texas 79409*

⁴⁰ *Istituto Nazionale di Fisica Nucleare, University of Trieste/ Udine, Italy*

⁴¹ *University of Tsukuba, Tsukuba, Ibaraki 305, Japan*

⁴² *Tufts University, Medford, Massachusetts 02155*

⁴³ *Waseda University, Tokyo 169, Japan*

⁴⁴ University of Wisconsin, Madison, Wisconsin 53706

⁴⁵ Yale University, New Haven, Connecticut 06520

Submitted to PRL, 12 July 2000

A full angular analysis has been performed for the pseudo-scalar to vector-vector decays $B^0 \rightarrow J/\psi K^{*0}$ and $B_s^0 \rightarrow J/\psi \phi$ to determine the amplitudes for decays with parity-even longitudinal (A_0) and transverse (A_{\parallel}) polarization and parity-odd transverse (A_{\perp}) polarization. The measurements are based on 190 B^0 candidates and 40 B_s^0 candidates collected from a data set corresponding to 89 pb^{-1} of $\bar{p}p$ collisions at $\sqrt{s} = 1.8 \text{ TeV}$ at the Fermilab Tevatron. In both decays the decay amplitude for longitudinal polarization dominates : $|A_0|^2 = 0.59 \pm 0.06 \pm 0.01$ for the B^0 decay and $|A_0|^2 = 0.61 \pm 0.14 \pm 0.02$ for the B_s^0 decay. The parity-odd amplitude is found to be small: $|A_{\perp}|^2 = 0.13_{-0.09}^{+0.12} \pm 0.06$ for B^0 and $|A_{\perp}|^2 = 0.23 \pm 0.19 \pm 0.04$ for B_s^0 .

PACS numbers: 13.20.He, 13.25.Hw

The decays $B^0 \rightarrow J/\psi K^{*0}$ and $B_s^0 \rightarrow J/\psi \phi$ are pseudo-scalar to vector-vector decays and in principle have three decay amplitudes which can be determined by studying the angular distributions of the final state particles. These decays can have orbital angular momenta between the J/ψ and K^* (or ϕ) of 0, 1, or 2, and three decay amplitudes govern these transitions. Another convenient description is given in the transversity basis [1,2] in which the decay amplitudes are defined in terms of the linear polarization of the vector mesons. In this basis the $L = 1$ (P wave) decays are governed by a single decay amplitude, A_{\perp} , corresponding to a parity-odd correlation between transversely polarized vector mesons. The other two decay amplitudes, A_0 and A_{\parallel} , are combinations of the parity-even $L = 0$ and $L = 2$ (S and D wave) decays. The longitudinal polarization fraction, as is commonly defined in the helicity basis [3], is given by $\Gamma_L/\Gamma = |A_0|^2$.

Determination of the decay amplitudes and phases probes the limitations of the factorization hypothesis [4]. Factorization assumes that a weak decay matrix element can be described as the product of two independent (hadronic) currents, in this case treating the J/ψ and $B \rightarrow K^*$ (ϕ) as currents. To the extent that factorization holds, final state interactions are negligible. The matrix elements factorize into short and long distance (weak and strong) parts and the polarization decay amplitudes do not interfere and so are expected to be relatively real.

A measurement of the parity-odd amplitude, A_{\perp} , is pertinent to studies of CP invariance. For example, if the decay $B^0 \rightarrow J/\psi K^{*0}$ (with $K^{*0} \rightarrow K_s^0 \pi^0$) were to occur mainly through either a parity-odd or even amplitude, then this mode could be used [1,5] as readily as the $B^0 \rightarrow J/\psi K_s^0$ decay mode for determining [6] the CP nonconserving parameter $\sin(2\beta)$. The situation holds as well for the decay $B_s^0 \rightarrow J/\psi \phi$, which is expected to have a very small CP decay rate asymmetry in the Standard (CKM) Model. In addition the polarization of the decay $B_s^0 \rightarrow J/\psi \phi$ is interesting for its potential to improve the precision of measurements of the lifetime difference between the B_s^0 mass eigenstates via an angular analysis [2,7].

The longitudinal polarization in $B^0 \rightarrow J/\psi K^{*0}$ was first measured by ARGUS [8] as ~ 1.0 followed by a CLEO [9] measurement of 0.8 ± 0.2 and a CDF (Collider Detector at Fermilab) measurement [10] of 0.65 ± 0.11 . A full angular analysis by CLEO [11] obtained a longitudinal polarization fraction of 0.52 ± 0.08 and a parity-odd fraction of 0.16 ± 0.09 . The only previous measurement of the B_s^0 decay mode, by CDF [10], obtained a longitudinal polarization fraction of 0.56 ± 0.21 , consistent with the results for B^0 as expected under $SU(3)$ -flavor symmetry.

This Letter describes a full angular analysis of both the B^0 and B_s^0 decay modes based on 89 pb^{-1} of $\bar{p}p$ collisions at $\sqrt{s} = 1.8 \text{ TeV}$ collected with the CDF detector at the Fermilab Tevatron. In this analysis, the $B^0 \rightarrow J/\psi K^{*0}$ and $B_s^0 \rightarrow J/\psi \phi$ decays are reconstructed from the decay modes $J/\psi \rightarrow \mu^+ \mu^-$, $K^{*0} \rightarrow K^+ \pi^-$, and $\phi \rightarrow K^+ K^-$. After the selection described below, there are 190 $B^0 \rightarrow J/\psi K^{*0}$ and 40 $B_s^0 \rightarrow J/\psi \phi$ candidates above background. The results presented here are independent of those in Ref. [10].

CDF is a general purpose detector and has been described in detail elsewhere [12]. For this analysis important elements of the detector are the silicon vertex detector, with track impact parameter resolution of $10 \mu\text{m}$, and the drift chamber, with charged particle momentum resolution of $\delta p_T/p_T \sim 0.001 p_T$, where p_T (in GeV/c) is the component of the momentum transverse to the $\bar{p}p$ collision axis. Chambers for muon detection provide coverage for particles with direction within 40 degrees of the transverse direction.

The event sample for this measurement is selected by online trigger and offline reconstruction criteria. The trigger signature is the decay of a J/ψ to two muons. Hits in the muon chambers forming a track segment consistent with a nominal muon transverse momentum $p_T > 3.0 \text{ GeV}/c$ satisfy the first level of the trigger. Candidate muon track segments must be separated by more than 10° in the plane transverse to the collision axis. The second level requires

drift chamber tracks, with $p_T > 2 \text{ GeV}/c$, which extrapolate to the track segments in the muon chambers. The third level accepts J/ψ candidates with a reconstructed mass between 2.8 and $3.4 \text{ GeV}/c^2$.

The offline reconstruction first selects J/ψ candidates. Two muons of opposite charge satisfying quality requirements are combined into a J/ψ candidate. A kinematic fit requiring the muons to originate from a common vertex is performed, and the confidence level of the fit is required to be at least 0.01. This results in a sample of about 290,000 candidate J/ψ 's.

Of these, candidates within $80 \text{ MeV}/c^2$ of the J/ψ mass ($3096.88 \text{ MeV}/c^2$) [13] are then combined with two oppositely charged tracks that form a K^* (ϕ) for the $B^0 \rightarrow J/\psi K^{*0}$ ($B_s^0 \rightarrow J/\psi \phi$) decays. CDF lacks the particle identification capability to distinguish between the two K - π charge assignments for a K^* candidate. However, the mass distribution for misidentified candidates is broader than the natural width of the K^* and their contribution is largely suppressed by choosing the assignment yielding a K^* mass closer to, and within $80 \text{ MeV}/c^2$ of, the world average ($896.1 \text{ MeV}/c^2$).

To further improve the signal to noise ratio, the B^0 candidate is required to have $p_T > 6.0 \text{ GeV}/c$, with the K^* having $p_T > 2.0 \text{ GeV}/c$. All four particles from the B^0 decay are required to come from a common ‘secondary’ vertex, with the confidence level of the fit being greater than 0.001. The proper decay length ($c \times$ proper decay time) for the B^0 is required to be at least $100 \mu\text{m}$. The resulting $K\pi\mu^+\mu^-$ mass distribution is plotted in Figure 1(a).

For the B_s^0 decay, the ϕ candidate is required to have a mass within $10 \text{ MeV}/c^2$ of the nominal ϕ mass ($1019.4 \text{ MeV}/c^2$). The narrow natural width of the ϕ provides for better background rejection than the K^* . In order to compensate for the lower expected yield of B_s^0 events, looser requirements are imposed: transverse momentum cuts of $1.5 \text{ GeV}/c$ and $4.5 \text{ GeV}/c$ are applied to the ϕ and B_s^0 candidates. The confidence level of the four track fit is again required to be greater than 0.001, and the proper decay length is required to be at least $50 \mu\text{m}$. The resulting $KK\mu^+\mu^-$ mass distribution is plotted in Figure 1(b).

The linear polarization of the vector mesons is determined from the angular distribution of the final state decay products. The decay angles are defined [2] as Θ_{K^*} , Θ_T , and Φ_T . In the rest frame of the K^* , Θ_{K^*} is the angle between the K momentum and the direction opposite the B meson (for the ϕ , the K^+ defines the angle). The transversity angles, Θ_T and Φ_T , are defined in the J/ψ rest frame: Θ_T is the angle between the μ^+ momentum and the perpendicular to the K^*-K plane; Φ_T is the azimuthal angle from the K^* to the projection of the μ^+ momentum onto the K^*-K plane.

The decay angular distribution is [7]:

$$\begin{aligned} d\Gamma/d\Omega \propto & 2 \cos^2 \Theta_{K^*} (1 - \sin^2 \Theta_T \cos^2 \Phi_T) |A_0|^2 \\ & + \sin^2 \Theta_{K^*} (1 - \sin^2 \Theta_T \sin^2 \Phi_T) |A_\parallel|^2 \\ & + \sin^2 \Theta_{K^*} \sin^2 \Theta_T |A_\perp|^2 \\ & + \frac{1}{\sqrt{2}} \sin 2\Theta_{K^*} \sin^2 \Theta_T \sin 2\Phi_T \operatorname{Re}(A_0^* A_\parallel) \\ & \mp \sin^2 \Theta_{K^*} \sin 2\Theta_T \sin \Phi_T \operatorname{Im}(A_\parallel^* A_\perp) \\ & \pm \frac{1}{\sqrt{2}} \sin 2\Theta_{K^*} \sin 2\Theta_T \cos \Phi_T \operatorname{Im}(A_0^* A_\perp) \end{aligned}$$

Normalization of the distribution to unity implies $|A_0|^2 + |A_\parallel|^2 + |A_\perp|^2 = 1$, and an unobservable phase is removed by requiring $\arg(A_0) = 0$. This leaves four measurable quantities: the polarization fractions, $\Gamma_L/\Gamma = |A_0|^2$ and $\Gamma_\perp/\Gamma = |A_\perp|^2$, and the phases of the matrix elements, $\arg(A_\parallel)$ and $\arg(A_\perp)$. The last two terms of the angular distribution have opposite signs for particle and anti-particle decay. The B^0 and \bar{B}^0 decays are flavor tagged by the charge of the K meson. The B_s^0 and \bar{B}_s^0 are not distinguishable by their final state particles, so for B_s^0 decays information about the phase of A_\perp is lost.

The matrix elements are extracted by fitting the observed decay angular distribution. The fit is performed over the decay angles and the B candidate mass range covered in Figure 1. To account for detector acceptance and selection criteria, Monte Carlo events are generated with detector and trigger simulations and processed by the same reconstruction software used on the data. The fit method uses an unbinned log-likelihood with the normalization depending on the parameters in the fit [14,15].

The background is modeled by a sum of polynomial terms of $\cos \Theta_{K^*}$ and $\cos \Theta_T$, and sines and cosines of Φ_T and $2\Phi_T$. The background angular distribution is determined from the events on both sides of the B meson mass peak.

Additional terms are included in the angular distribution to account for the residual probability ($\sim 6\%$) of misidentifying the final state hadrons in the selected $B^0 \rightarrow J/\psi K^{*0}$ decays. Events reconstructed under the wrong hypothesis will yield incorrect decay angles having a distribution different from, but fully correlated with, the polarized decay distribution. The augmented likelihood function corrects for the effect based on the kinematics as determined from Monte Carlo.

The results from the global fit are illustrated in Figure 2. The independent variables are functions of the transversity angles: $\cos \Theta_{K^*}$, $\cos \Theta_T$, and Φ_T . The points are the background subtracted projection of the data corrected for

detector and reconstruction efficiencies. The superimposed curves, derived from the results of the global fit, are in good agreement with the data.

Sources of systematic uncertainty are, in order of importance, the model of the background shape, Monte Carlo B generation parameters, trigger simulation, and B^0 - B_s^0 cross talk. The last two are found to have negligible contribution. The uncertainty of the final result is still dominated by the statistics of the event sample [14].

The underlying background shape is not known from first principles. To estimate the systematic uncertainty from the background modelling, multiple fits with different parametrizations of the background decay angles were studied. Different models of the shape are sensitive to different inaccuracies of the background shape function, and the spread in the fitted values is used to estimate the sensitivity to possibly unaccounted structure.

The input parameters to the Monte Carlo generation of B mesons are the b quark mass and generation mass scale, the parton distribution functions and fragmentation parameters. The effect on the measurement is determined by varying the parameters by their nominal uncertainties and refitting for the decay amplitudes. Systematic uncertainties due to the modeling of the trigger selection criteria are studied in a similar fashion.

The similarity of the decay kinematics for the B^0 and B_s^0 decays allows for a possible cross contamination through K - π misidentification. Monte Carlo studies give contamination fractions of 2.1% (4.4%) in the B^0 (B_s^0) sample. The assigned systematic uncertainty is equal to the difference in the B^0 and B_s^0 polarization fraction, multiplied by the contamination fraction.

The final results of this analysis are summarized in Table I, and are illustrated in Figure 3. For the $B^0 \rightarrow J/\psi K^*$ the magnitudes of decay amplitudes are in good agreement with the results from CLEO [11]. The longitudinal polarization fraction dominates: $\Gamma_L/\Gamma = |A_0|^2 = 0.59 \pm 0.06 \pm 0.01$ and the parity-odd fraction is small: $\Gamma_\perp/\Gamma = |A_\perp|^2 = 0.13^{+0.12}_{-0.09} \pm 0.06$. In contrast to the CLEO result, the CDF measurement for the phase of A_\parallel favors the presence of strong final state interactions, in as much as $\arg(A_\parallel)$ is not close to 0 or π . However, the results from the two experiments are not inconsistent, given their uncertainties. The results for the $B_s^0 \rightarrow J/\psi \phi$ are the first available from a full angular analysis. The B_s^0 results also show a dominant longitudinal polarization fraction $\Gamma_L/\Gamma = |A_0|^2 = 0.61 \pm 0.14 \pm 0.02$ and a small parity-odd fraction: $\Gamma_\perp/\Gamma = |A_\perp|^2 = 0.23 \pm 0.19 \pm 0.04$, consistent with the B^0 results and SU(3) flavor symmetry.

We thank the Fermilab staff and the technical staffs of the participating institutions for their vital contributions. This research was supported by the U. S. Department of Energy and the National Science Foundation; the Italian Istituto Nazionale di Fisica Nucleare; the Ministry of Education, Science and Culture of Japan; the Natural Sciences and Engineering Research Council of Canada; the National Science Council of the Republic of China; the Swiss National Science Foundation; the A. P. Sloan Foundation; and the Bundesministerium für Bildung und Forschung, Germany. We thank H. Lipkin for bringing the transversity basis to our attention and acknowledge illuminating correspondence and discussions with I. Dunietz and J. Rosner.

- [1] I. Dunietz *et al.*, Phys. Rev. D**43**, 2193 (1991).
- [2] A.S. Dighe *et al.*, Phys. Lett. B**369**, 144 (1996).
- [3] G. Valencia, Phys. Rev. D**39**, 3339 (1989); G. Kramer and W.F. Palmer, Phys. Rev. D**45**, 193 (1992); B.F.L. Ward, Phys. Rev. D**45**, 1544 (1992).
- [4] M. Bauer, B. Stech and M. Wirbel, Z. Phys. C**29**, 637 (1985), C**34**, 103 (1987); M. Gourdin, A.N. Kamal and X.Y. Pham, Phys. Rev. Lett. **73**, 3355 (1994); R. Aleksan *et al.*, Phys. Rev. D**51**, 6235 (1995); H.Y. Cheng, Phys. Lett. B**395**, 345 (1997); F.M. Al-Shamali and A.N. Kamal, Eur. Phys. J. C**4**, 669 (1998) and Phys. Rev. D**60**, 114019 (1999).
- [5] B. Kayser *et al.*, Phys. Lett. B**237**, 508 (1990).
- [6] T. Affolder *et al.*, Phys. Rev. D**61**, 072005 (2000).
- [7] A.S. Dighe, I. Dunietz and R. Fleischer, Eur. Phys. J. C **6**, 647 (1999); A. Dighe and S. Sen, Phys. Rev. D**59**, 074002 (1999).
- [8] H. Albrecht *et al.*, Phys. Lett. B**340**, 217 (1994).
- [9] M.S. Alam *et al.*, Phys. Rev. D**50**, 43 (1994).
- [10] F. Abe *et al.*, Phys. Rev. Lett. **75**, 3068 (1995).
- [11] C.P. Jessop *et al.*, Phys. Rev. Lett. **79**, 4533 (1997).
- [12] F. Abe *et al.*, Nucl. Inst. and Meth. A**271**, 387 (1988), Phys. Rev. D**50**, 2966 (1994) and Phys. Rev. Lett. **74**, 2626 (1995).
- [13] C. Caso *et al.*, Euro. Phys. J. C**3**, 1 (1998).
- [14] S.P. Pappas, Ph.D. dissertation, Yale University (1999).

[15] F. DeJongh, Ph.D. dissertation, California Institute of Technology (1996); D. Coffman *et al.*, Phys. Rev. D45, 2196 (1992).

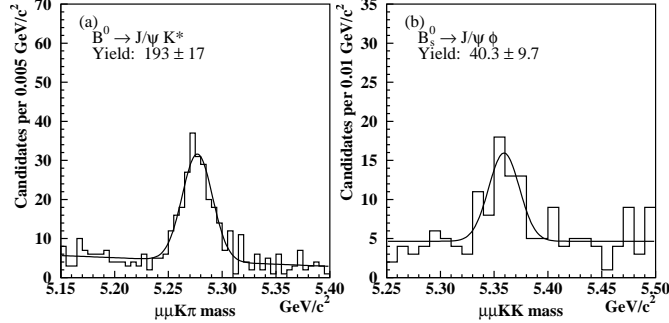


FIG. 1. Invariant mass distributions, after all selection requirements, for (a) $B^0 \rightarrow J/\psi K^{*0}$ and (b) $B_s^0 \rightarrow J/\psi \phi$ candidates.

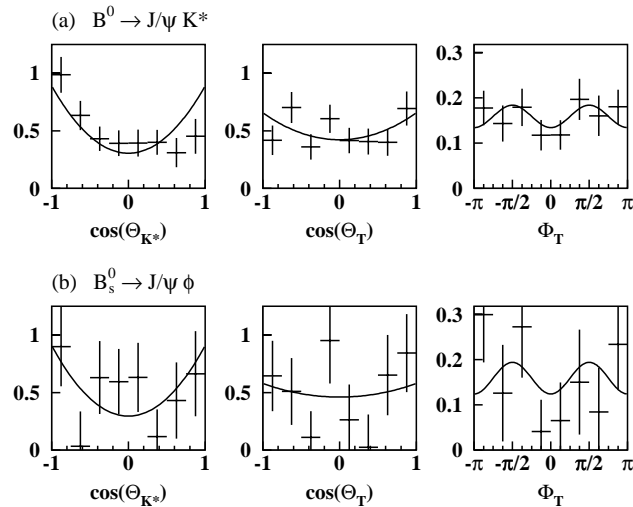


FIG. 2. Projections of the results from the full angular fit and the background subtracted data, corrected for acceptance, are shown for each of the decay angles, for (a) the $B^0 \rightarrow J/\psi K^{*0}$ mode and (b) the $B_s^0 \rightarrow J/\psi \phi$ mode.

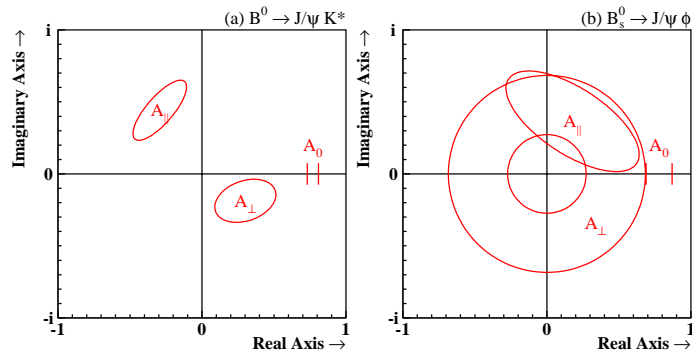


FIG. 3. One standard deviation contours, including statistical and systematic uncertainties, for the fitted decay amplitudes in the complex plane, for (a) $B^0 \rightarrow J/\psi K^{*0}$ and (b) $B_s^0 \rightarrow J/\psi \phi$ decays.

Quantity	$B^0 \rightarrow J/\psi K^{*0}$	$B_s^0 \rightarrow J/\psi \phi$
A_0	$0.77 \pm 0.04 \pm 0.01$	$0.78 \pm 0.09 \pm 0.01$
A_{\parallel}	$0.53 \pm 0.11 \pm 0.04$	$0.41 \pm 0.23 \pm 0.05$
$\arg(A_{\parallel})$	$2.2 \pm 0.5 \pm 0.1$	$1.1 \pm 1.3 \pm 0.2$
A_{\perp}	$0.36 \pm 0.16 \pm 0.08$	$0.48 \pm 0.20 \pm 0.04$
$\arg(A_{\perp})$	$-0.6 \pm 0.5 \pm 0.1$	
$\Gamma_L/\Gamma = A_0 ^2$	$0.59 \pm 0.06 \pm 0.01$	$0.61 \pm 0.14 \pm 0.02$
$\Gamma_{\perp}/\Gamma = A_{\perp} ^2$	$0.13^{+0.12}_{-0.09} \pm 0.06$	$0.23 \pm 0.19 \pm 0.04$

TABLE I. Fitted decay amplitudes and phases (in radians). The uncertainties are statistical and systematic, respectively.